e-mail: peter.mcleod@psy.ox.ac.uk
†Department of Experimental Psychology, University of Sussex, Falmer, Brighton BN1 9QG, UK

1. Land, M. F. & Collett, T. S. *J. Comp. Physiol.* **89,** 331–357 (1974).
2. Land, M. F. & McLeod, P. *Nature Neurosci.* **3,** 1340–1345 (2000).
3. McLeod, P., Reed, N. & Dienes, Z. *J. Exp. Psychol. Hum. Percept. Perf.* (submitted).
4. McLeod, P., Reed, N. & Dienes, Z. *J. Exp. Psychol. Hum. Percept. Perf.* **27,** 1347–1355 (2001).
5. Tresilian, J. *Q. J. Exp. Psychol.* **48,** 688–715 (1995).

Competing financial interests: declared none.

Flightless birds

When did the dodo become extinct?

The extinction of the dodo (*Raphus cucullatus* L.; Fig. 1) is commonly dated to the last confirmed sighting in 1662, reported by Volkert Evertsz on an islet off Mauritius[1,2]. By this time, the dodo had become extremely rare — the previous sighting having been 24 years earlier — but the species probably persisted unseen beyond this date. Here we use a statistical method to establish the actual extinction time of the dodo as 1690, almost 30 years after its most recent sighting.

In most cases, the extinction of a species must be inferred from the record of sightings or from collections of individual organisms. But when a species becomes increasingly rare before its final extinction, it may continue to exist unseen for many years — so the time of its last sighting may be a poor estimate of the time of extinction.

We applied an optimal linear estimation method based on the sighting record of the dodo to determine when the bird finally became extinct. Let $T_1 > T_2 > \ldots > T_k$ be the k most recent sighting times of a species, ordered from most recent to least recent. Interest centres on using this record to estimate the extinction time, θ. In this context, optimal linear estimation is based on the remarkable result that the joint distribution of the k most recent sighting times has (at least roughly) the same 'Weibull form', regardless of the parent distribution of the complete sighting record[3].

Briefly, the optimal linear estimator of θ has the form of a weighted sum of the sighting times, calculated as

$$\hat{\theta} = \sum_{i=1}^{k} a_i T_i$$

The vector of weights is given by

$$a = (e^t \Lambda^{-1} e)^{-1} \Lambda^{-1} e$$

where e is a vector of k 1's and Λ is the symmetric $k \times k$ matrix with typical element $\lambda_{ij} = (\Gamma(2\hat{\nu}+i)\Gamma(\hat{\nu}+j))/(\Gamma(\hat{\nu}+i)\Gamma(j))$, $j \leq i$, and where Γ is the standard gamma function. Also,

$$\hat{\nu} = \frac{1}{k-1} \sum_{i=1}^{k-2} \log \frac{T_1 - T_k}{T_1 - T_{i+1}}$$

is an estimate of the shape parameter of the joint Weibull distribution of the k most recent sighting times. An approximate $1-\alpha$ confidence interval for θ is given by

$$\left(T_1 + \frac{T_1 - T_k}{S_L - 1}, T_1 + \frac{T_1 - T_k}{S_U - 1}\right)$$

where $S_L = (-\log(1-\alpha/2)/k)^{-\hat{\nu}}$ and $S_U = (-\log(\alpha/2)/k)^{-\hat{\nu}}$.

The $k = 10$ most recent confirmed sighting times of the dodo are 1662, 1638, 1631, 1628, 1628, 1611, 1607, 1602, 1601 and 1598.

An escaped slave named Simon claimed to have seen a dodo as recently as 1674. However, the reliability of this and other later claims are open to question. For this record, the estimated shape parameter is $\hat{\nu} = 0.39$ and the estimated extinction time is $\hat{\theta} = 1690$. The approximate 0.95 confidence interval for θ is (1669, 1797). The width of this interval is a result of the low sighting rate of the dodo at the end of its sighting record. Because this rate was so low, it is impossible to rule out an extinction date as late as 1797. This implies that the purported sighting in 1674 cannot be ruled out on the basis of extinction time alone. If a sighting in 1674 is included in the record, the estimated extinction time is extended only modestly to 1700 and actually narrows the confidence interval to (1679, 1790).

David L. Roberts*, Andrew R. Solow†
**Royal Botanic Gardens, Kew, Richmond, Surrey TW9 3AE, UK*
†Woods Hole Oceanographic Institution, Woods Hole, Massachusetts 02543, USA
e-mail: asolow@whoi.edu

1. Cheke, A. S. in *Studies of Mascarene Island Birds* (ed. Diamond, A. W.) 5–89 (Cambridge Univ. Press, Cambridge, 1987).
2. Fuller, E. *Dodo: A Brief History* (Universe Books, New York, 2002).
3. Cooke, P. *Biometrika* **67,** 257–258 (1980).

Competing financial interests: declared none.

Figure 1 Dead as a dodo: the flightless bird from Mauritius and the adjacent islands weighed in at about 23 kg and was hunted to extinction. Its last confirmed sighting was in 1662, although an escaped slave claimed to have seen the bird as recently as 1674. In fact, it is estimated by using a Weibull distribution method that the dodo may have persisted until 1690, almost 30 years after its presumed extinction date. Although gone forever, the dodo's lumbering appearance in Lewis Carroll's *Alice's Adventures in Wonderland* has ensured that it will not be forgotten.

COMMUNICATIONS ARISING

Astronomy

Black holes, fleas and microlithography

Fresnel lenses allow almost perfect imaging in widely different circumstances, but their focus is perfect only for a single wavelength. Wang *et al.*[1] have shown how the effective bandpass may be widened for X-ray microscopy by using a compound diffractive/refractive lens near to an absorption edge. A compound lens has also been proposed for high-energy astronomy, working well above all absorption edges[2,3]. Although the scale is very different, we point out here that the principle is the same. Ever since Galileo constructed an astronomical telescope that he was able to reconfigure to study fleas and gnats, astronomy and microscopy have relied on optics that are closely related, but different in detail.

In principle, the highest resolution in each case is obtained with the shortest wavelengths — X-rays or γ-rays. In microscopy and microlithography, the spatial resolution of the optical system dictates the level of detail in images and the fineness of structures in integrated circuits. Resolution better than 30 nm has been reported[4]

— a value that is close to the theoretical limit.

In astronomy, it is angular resolution that is important. For X-rays, the best available angular resolution (0.5 arc seconds (arcsec) with the Chandra observatory[5]) is about 10^4 times worse than the diffraction limit. There are good reasons for trying to do better: attaining one of astronomy's 'holy grails' — to 'see' a black hole by imaging the space-time around the supermassive objects at the centres of active galaxies — would require resolution below 1 micro-arcsec, corresponding to the diffraction limit for a 60-cm-diameter system using 500-keV γ-rays, or a 60-m-diameter one using 5-keV X-rays.

In microscopy, the best resolution is obtained using Fresnel zone plates and the closely related phase Fresnel lenses. These are highly chromatic, with a focal length that is inversely proportional to wavelength, so the best resolution is obtained with essentially monochromatic radiation. Wang *et al.*[1] have proposed a scheme for making an achromatic X-ray lens by combining a Fresnel lens with a refractive component (Fig. 1). Such lenses should have the same high resolution but with a larger useful bandwidth.

Fresnel lenses have also been considered for high-energy astronomy[2,3,6], and the achromatic Fresnel lens scheme suggested by Wang *et al.* has also been proposed in that context[3]. Figure 1 shows a general achromatic lens scheme of this type. It has even been shown (L. Speybroeck, unpublished work, and ref. 6) that the second derivative of focal length, as well as the first, can be corrected by separating the two components — a configuration that may also find application in microscopy.

The achromatic configuration proposed for microscopy differs in one detail. Wang *et al.* suggest taking advantage of the high dispersion that occurs close to X-ray absorption edges. Over wider bands and for short wavelengths, λ, the dispersion, D, that they define is close to zero, but correction remains possible because of the λ^{-2} component in the expression for the focal length, f. The radii of curvature of the refractive components are much less favourable, but in astronomy the considerations are different. Spatial resolution, which is of interest in microscopy, depends on $\lambda f/d$, where d is the diameter of the lens, whereas angular resolution depends only on λ/d. Thus, long focal lengths can be used for astronomy, minimizing both the chromatic aberration that requires correction and the curvature of the components needed to correct it. Furthermore, with large d and short λ, micro-arcsec resolution does not necessarily require perfect phase coherence.

Building a micro-arcsec telescope based on a Fresnel lens will not be easy. The focal length could be up to a million kilometres, and two or three separate satellites carrying the lens(es) and the focal plane array will have to be positioned with centimetre accuracy. But micro-arcsec imaging is an important target (NASA recently included a black-hole imager in its SEUS Roadmap[7]) and other approaches to achieving this goal, such as an X-ray interferometer carried on a flotilla of spacecraft[8,9], have requirements that are just as extreme, if not more so.

Although overall system performance, including spacecraft positioning for example, will have to be taken into account, for Fresnel-lens-based telescopes the purely optical performance can be predicted with confidence. The basic physical principle has already been demonstrated in microscopy, where achromatic lenses will presumably also soon come into use. The different requirements of astronomy merely require a change of scale: lenses of many metres in diameter with millimetre-scale zones, instead of sub-millimetre lenses with zones of the order of 50 nm (Table 1). Constructional tolerances will be correspondingly easier to achieve.

An achromatic Fresnel-lens telescope measuring 10^{11} m in length will certainly not be built very soon. Perhaps experience with lenses that are limited by diffraction at the nanometre scale will give us the confidence to proceed to imaging black holes with millions of times the mass of our Sun.

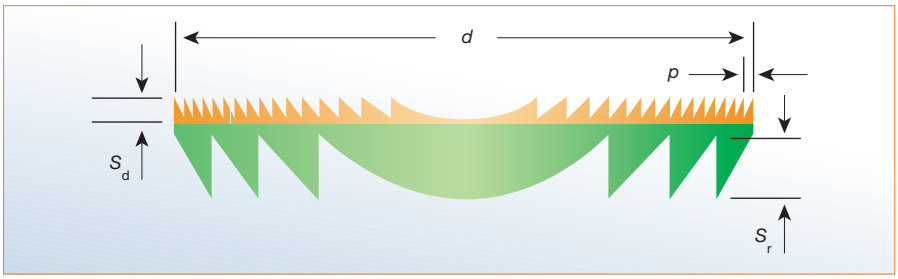

Figure 1 An achromatic refractive/diffractive lens. The diffractive component (orange) could be a phase Fresnel lens (as shown) or a (phase) zone plate. The refractive component (green) is stepped to avoid excessive absorption. Its curvature is exaggerated here for clarity. The same principle can be used both in astronomy[3] and in microscopy/microlithography[1], but with different parameters (Table 1). In the microscope objective case, stepping the refractive component introduces no error; in the astronomical case, some resolution is lost, but multiple passbands increase the throughput. d, Diameter of the lens; S_d and S_r are the depth of the steps in the diffractive and refractive components, respectively, and correspond to phase shifts of an integer number of cycles at the nominal wavelength; p is the finest pitch of the diffractive element.

Table 1 Lens parameters for astronomy and microscopy/microlithography

	Astronomy[3]	*Microscopy*[1]
Lens diameter	5 m	1 mm
Focal length at nominal wavelength	+40,000 km	+22.475 mm
Wavelength, λ (photon energy)	0.062 nm (20 keV)	1.335 nm (929 eV)
Theoretical resolution	5×10^{-6} arcsec	35 nm
Diffractive component		
Pitch at edge	0.5 mm	60 nm
Focal length	+20,000 km	+22.475 mm
Refractive component		
Material	Polycarbonate	Copper
Focal length	−40,000 km	–
Maximum thickness*	20 mm	<1 μm

Apart from the obviously disparate scales, the differences are driven by the dispersion $Z=(\mathrm{d}\delta/\mathrm{d}\lambda)(\lambda/\delta)$, where $\delta=1-\mu$ and μ is the refractive index. We adopt this measure of dispersion instead of the parameter $D=\mathrm{d}f_i/\mathrm{d}\lambda$ used in ref. 1 as it includes the dispersion present even at short wavelengths, where the atomic scattering factor f_1 is constant. Well above absorption edges (astronomy), Z is very close to −2, independent of the material. In the band close to the copper L absorption edge (microscopy/microlithography), Z is large and varies in the range −800 to +250.
*Based on 50% mean transmission.

Gerry Skinner*, Paul Gorenstein†
**Centre d'Étude Spatiale des Rayonnements, Toulouse 31208, France*
e-mail: skinner@cesr.fr
†Harvard-Smithsonian Center for Astrophysics, Cambridge, Massachusetts 02138, USA

1. Wang, Y., Yun, W. & Jacobsen, C. *Nature* **424,** 50–53 (2003).
2. Skinner, G. K. *Astron. Astrophys.* **375,** 691–700 (2001).
3. Skinner, G. K. *Astron. Astrophys.* **383,** 352–359 (2002).
4. Gil, D., Menon, R. & Smith, H. I. *J. Vac. Sci. Tech. B* (in the press).
5. Jerius, D. *et al. Proc. SPIE* **4012,** 17–27 (2000).
6. Gorenstein, P. *Proc. SPIE* **4851,** 599–606 (2003).
7. NASA Structure and Evolution of the Universe Subcommittee. *Beyond Einstein: From the Big Bang to Black Holes* (NASA, 2003).
8. White, N. *Nature* **407,** 146–147 (2000).
9. Cash, W. *Proc. SPIE* **4852,** 196–209 (2003).

erratum

Mechanism for 'superluminal' tunnelling

Herbert G. Winful

Nature **424,** 638 (2003)

The following information was omitted from Fig. 1 of this communication: time is in units of the transit time, L/c, through an equivalent distance *in vacuo*; the brown curve is the incident pulse and the blue curve represents the tunnelled pulse; also, the tunnelled pulse has been scaled by a factor of 1/0.0014 to make it visible.